applied sciences

MDPI

Article

Myo/Nog Cells Increase in Response to Elevated Intraocular Pressure and Mitigate Ganglion Cell Death in a Mouse Model of Glaucoma

Paul Lecker [1], Karanveer Johal [1], Alexa McGrath [1], John Spikes II [1], Jake Bernstein [1], Victoria MacPherson [1], Rushil Brahmbhatt [1], Nada Fadl [1], Edgar Weyback-Liogier [1], Sarah Adams [1], Rachel Souza [1], E-Jine Tsai [1], Mark Martin [1], Jacquelyn Gerhart [1], Grezgorz Gorski [1], Federica De Cecco [2], Brian Heist [1], Sebastian Egberts [1], Mindy George-Weinstein [1] and Arturo Bravo-Nuevo [1,*]

[1] Philadelphia College of Osteopathic Medicine, 4170 City Ave, Philadelphia, PA 19131, USA; kj253700@pcom.edu (K.J.); js7534@pcom.edu (J.S.II); ew218176@pcom.edu (E.W.-L.); sa73572@pcom.edu (S.A.); mam898@cabrini.edu (M.M.)

[2] Department of Innovative Technologies in Medicine & Dentistry, University "G. d'Annunzio" Chieti-Pescara, Via dei Vestini 31, 66100 Chieti, Italy; federica.dececco@unich.it

* Correspondence: arturobr@pcom.edu

Abstract: Glaucoma is one of the leading causes of blindness worldwide. Decreased aqueous humor drainage causes an increase in intraocular pressure (IOP), which in turn damages the ganglion cells of the retina and optic nerve. A mouse model of glaucoma was used to examine the behavior of Myo/Nog (M/N) cells, which were previously shown to respond to cataract surgery and retinopathy induced by hypoxia, light damage, and intravitreal injection of human retinal pigment epithelial cells. M/N cells express the skeletal-muscle-specific transcription factor MyoD, the bone morphogenetic protein inhibitor Noggin, and brain-specific angiogenesis inhibitor 1 (BAI1). Glaucoma was induced by injecting microbeads into the anterior chamber (AC) of the right eye to obstruct the flow of aqueous humor into the trabecular meshwork. IOP was elevated within three days of addition of microbeads. Loss of retinal ganglion cells (RGCs) and thinning of the ganglion cell layer–nerve fiber layer (GCL-NFL) was observed in tissue sections by day 32. The injection of microbeads resulted in an increase in BAI1-positive (+) M/N cells in the trabecular meshwork, ciliary body, canal of Schlemm, cornea, and ganglion cell layer (GCL). M/N cells ingested microbeads. The effect of further increasing the population of M/N cells on IOP and RGC loss was determined by injecting BAI1+ cells isolated from the brain into the AC of both eyes. Exogenous M/N cells prelabeled with CellTracker™ Red were found in the same tissues as the endogenous population of M/N cells in eyes with and without elevated IOP. The addition of M/N cells did not significantly reduce IOP in bead-injected eyes. However, there were significantly more RGCs and the NFL was thicker in glaucomatous eyes with M/N cell supplementation than eyes injected with phosphate-buffered saline. The numbers of RGCs and NFL thickness were similar in glaucomatous and non-glaucomatous eyes after adding M/N cells. These results demonstrate that endogenous M/N cells respond to elevated IOP in the anterior and posterior segments in response to induction of glaucoma. M/N cells' mitigation of RGC loss may reflect a neuroprotective effect within the retina, as opposed to a significant drop in IOP.

Keywords: glaucoma; intraocular pressure; Myo/Nog cells; retinal ganglion cells

Citation: Lecker, P.; Johal, K.; McGrath, A.; Spikes, J., II; Bernstein, J.; MacPherson, V.; Brahmbhatt, R.; Fadl, N.; Weyback-Liogier, E.; Adams, S.; et al. Myo/Nog Cells Increase in Response to Elevated Intraocular Pressure and Mitigate Ganglion Cell Death in a Mouse Model of Glaucoma. *Appl. Sci.* **2023**, *13*, 12423. https://doi.org/10.3390/app132212423

Academic Editor: Darin Zerti

Received: 31 August 2023
Revised: 11 November 2023
Accepted: 15 November 2023
Published: 17 November 2023

1. Introduction

Glaucoma is the leading cause of irreversible blindness worldwide [1]. Disease progression is usually insidious, eventually leading to a loss of peripheral vision and, when untreated, blindness [2–11]. The pathophysiology of glaucoma involves damage to the optic nerve that usually results from an increase in intraocular pressure (IOP) [1,2]. In closed-angle glaucoma, the clinical presentation is typically acute, with pain and loss of

vision from pupillary dilation or lens dislocation into the iris [12–15]. Drainage of aqueous humor is impaired, leading to severely elevated IOP [1,16], resulting in ganglion cell death and subsequent blindness. By contrast, open-angle glaucoma typically presents asymptomatically and progresses more slowly than closed-angle glaucoma. In this case, the aqueous humor outflow at Schlemm's canal is impeded by pathologic resistance in the trabecular meshwork or uveoscleral outflow [17,18]. The subsequent accumulation of fluid increases IOP, leading to retinal ganglion cell (RGC)death, axonal thinning, optic nerve cupping, and loss of vision [19–25].

Mouse models of glaucoma are useful for identifying factors involved in the elevation of IOP and testing potential therapeutic interventions. One such model involves the injection of microbeads into the anterior chamber (AC) of the murine eye. Microbeads impede outflow at the canal of Schlemm [26,27], thereby replicating the pathophysiology of open-angle glaucoma. Increased IOP causes progressive loss of RGCs that plateaus approximately three weeks after bead injection [26,27].

In this study, we examined the behavior of Myo/Nog (M/N) cells in a modified version of this murine glaucoma model. M/N cells were named for their expression of MyoD, a skeletal-muscle-specific transcription factor, and Noggin, an inhibitor of bone morphogenetic proteins [28–34]. M/N cells also express brain-specific angiogenesis inhibitor 1 (BAI1) [35]. They are typically present in low numbers within the eye under normal conditions [30,36–41]. Injury to the retina or lens activates M/N cells, stimulating their proliferation and migration to wounds, and, in some cases, promotes their differentiation into contractile myofibroblasts [37–39,42–45]. Depletion of M/N cells in a model of oxygen-induced retinopathy (OIR) led to increased photoreceptor cell death [38], whereas intravitreal injection of M/N cells isolated from murine brains into the light-damaged retina actually reduced photoreceptor cell loss and preserved function [39]. Similarly, cell death was decreased when M/N cells were injected into the site of focal brain injury [46].

The following study was undertaken to examine the behavior of endogenous M/N cells in the anterior and posterior segments in response to elevated IOP. Also tested were the effects of adding brain-derived (donor) M/N cells to the AC on IOP, RGC loss, and thinning of the nerve fiber layer (NFL) of the retina.

2. Methods

2.1. Animals

Male and female C57BL/6J mice sourced from Jackson Laboratories (Bar Harbor, ME, USA) were raised from birth in controlled conditions (12–12 h light/dark schedule at 5–8 lux) until three to five months of age. All procedures utilized were in accordance with the Association for Research in Vision and Ophthalmology's (ARVO) Statement for the Use of Animals in Ophthalmic and Vision Research and were approved (Protocol #A17-012) by the Philadelphia College of Osteopathic Medicine's Institutional Animal Care and Use Committee (IACUC).

2.2. Induction of Glaucomatous State

IOP was elevated in the right eye with a modification of the method described by Ito et al. (2006) and Samsel et al. [26,27]. Just prior to microbead injection, mice were anesthetized via administration of an 87.5 mg/Kg ketamine/12.5 mg/Kg xylazine mixture. The ACs of the right eyes of the anesthetized mice were injected with a 2 µL solution of 4.5 µm magnetic polystyrene microbeads (Invitrogen Dynabeads™ M-450 Epoxy, Thermo Fisher Scientific, Waltham, MA, USA) suspended in phosphate-buffered saline (PBS) (1.6×10^6 beads/µL) with a 10 µL Gastight Hamilton syringe (Hamilton Company, Reno, NV, USA). The epoxy coating was removed from the beads prior to their injection [26]. A hand-held magnet was used to attract the beads to the iridocorneal angle (Figure 1A). The left eyes were used for intra-animal controls. IOP was measured using a Tonopen (Icare, Raleigh, NC, USA) five minutes after administration of the ketamine cocktail. Subsequent IOP measurements occurred on days (D) 4, 7, 14, 21, and 28 in both the right

(glaucomatous) and left (non-glaucomatous) eyes (Figure 1B). An increase in IOP of more than 30% in the right eye on D7 compared to D0 was considered a successful glaucoma induction procedure.

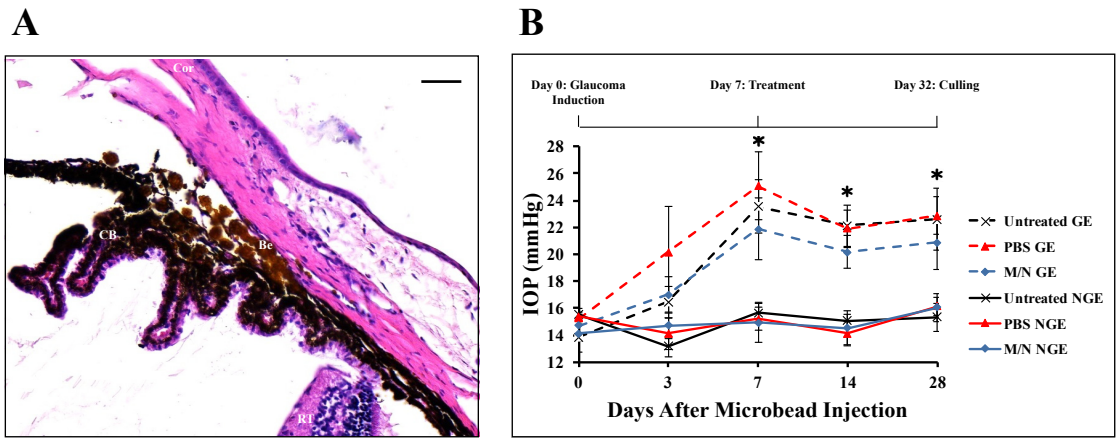

Figure 1. Induction of high IOP through intraocular injection of microbeads. (**A**) Sections of the iridocorneal angle of eyes were stained with H&E on D32 after injection of microbeads. The beads appear brown in tissue sections. Cor, CB, Be, and RT are the cornea, ciliary body, microbeads, and retina, respectively. Scale bar represents 45 µm. (**B**) Intraocular pressure data from each treatment group in eyes with and without bead injections (hatched lines and solid lines, respectively). Untreated eyes received no injections. Injection of beads significantly elevated the IOP (Asterisk means a $p \leq 0.05$) in all three groups by D3 in the glaucomatous right eyes (GEs) compared to their non-glaucomatous left eyes (NGEs).

2.3. M/N Cell Extraction and Labeling

Primary M/N cells were isolated from C57BL/6J donor mouse brains according to protocols described previously [39,46]. Briefly, the donor's brain was sliced into small pieces and incubated in 0.25% Trypsin-EDTA (Thermo Fisher Scientific, Waltham, MA, USA) at 37 °C for 15 min. A single-cell suspension was produced through trituration. The population that non-specifically bound magnetic anti-mouse IgM secondary antibodies was removed from the cell sorting column (Miltenyi Biotec, Auburn, CA, USA). The remaining cells were incubated with the G8 anti-BAI1 monoclonal antibody (mAb) and magnetic anti-IgM secondary antibodies (Miltenyi Biotec). Bound, BAI1-positive cells were eluted from the column in buffer according to the manufacturer's instructions. Donor M/N cells were labeled with CellTracker™ Red CMTPX fluorescent labeling dye (Invitrogen, Carlsbad, CA, USA) [47]. Then, 2 µL of PBS containing 6000 pre-labelled M/N cells was injected into both eyes of five mice on D7 using a 10 µL Gastight Hamilton syringe. Five control mice received an injection of 2 µL of PBS.

2.4. Treatment Groups

All subjects were anesthetized with an 87.5 mg/Kg ketamine–12.5 mg/Kg xylazine mixture. Five mice in three of the four treatment groups received bilateral AC injections with a gas-tight syringe. Group 1 (treatment) received 2 µL of 6000 brain-derived M/N cells. Group 2 (vehicle control) received 2 µL of PBS. Group 3 (no treatment) did not receive AC injections. IOP was serially measured weekly as described above.

2.5. Embedding and Sectioning

Mice were euthanized on D32. Eyes were enucleated, washed in PBS, and fixed in 4% formaldehyde overnight. Eyes were embedded in paraffin as described previously utilizing a Lynx II tissue processor (Electron Microscopy Sciences, Hatfield, PA, USA) [28,30]. Then, 8 µM sections were obtained with the Epredia HM 355S microtome (Fisher Scientific, Waltham, MA, USA).

2.6. Quantitation of RGCs and Measurement of GCL-NFL Thickness

Tissue sections were stained with hematoxylin 2 and eosin-Y (H&E) (Richard Allan Scientific, Kalamazoo, MI, USA). The number of RGCs was counted in five sections per eye in the first three fields on either side of the optic nerve at 60× magnification. The GCL-NFL/inner nuclear layer (INL) thickness ratio was quantified in these sections using the measuring tool available in NIS Elements software (https://www.microscope.healthcare.nikon.com/products/software/nis-elements accessed on 30 August 2023, Nikon Inc., Melville, NY, USA). Measurements were compared in five sections from the GEs and NGEs. RGCs were distinguished from microglia, astrocytes, and displaced amacrine cells by nuclear size and morphology. However, we did not label the GCL with a specific antibody against them.

2.7. Immunofluorescence Microscopy

Sections were incubated with 0.9 µg/mL of the G8 mAb against BAI1 to detect M/N cells as described previously [29,35,38]. BAI1 mAb binding was visualized with 2 µg/mL goat anti-mouse IgM secondary antibody conjugated with anti-goat Alexa Fluor 488 (1:400 dilution in 10% goat serum in PBS). Slides were cover-slipped with Fluorogel-II containing 4′,6-diamidino-2-phenylindole (DAPI) (Electron Microscopy Sciences, Hatfield, PA, USA).

Quantitation of M/N cells throughout the eye was accomplished with the Nikon Eclipse E800 epifluorescence microscope and NIS elements software (Nikon Inc.). RGCs and the NFL/INL ratio were quantified in the glaucomatous and non-glaucomatous eyes of the same mouse to compare the quantity and locations of M/N cells. Distinction between endogenous and exogenous M/N cells was made by quantifying cells labeled with Alexa 488 only (endogenous cells) and Alexa 488 plus CellTracker™ Red CMTPX dye (exogenous cells).

2.8. Statistical Analyses

Data are reported as the means and standard deviations (SDs) within each group. One-way ANOVA analyses were conducted with double-tailed t-tests to evaluate statistical significance between treatment groups and controls for the numbers of M/N and RG cells, and the NFL/IFL ratios. $p < 0.05$ was considered statistically significant. Calculations were performed with Microsoft Excel (Microsoft, Redmond, WA, USA).

3. Results

3.1. Effect of Injecting Beads into the AC on IOP

Histological analysis showed that the beads were present within the iridocorneal angle and appeared lodged within the trabecular meshwork (Figure 1A). Introducing beads into the right eye's AC resulted in increased IOP across all three treatment groups within three days of their injection (Figure 1B). The increase in IOP peaked 7 days after the injection of the beads and remained elevated through D28 (Figure 1B). No significant differences in IOP were observed between the different treatment groups.

3.2. Effects of Elevated IOP on the Retina

The number of RGCs and the thickness of the NFL, given as NFL/INL ratio, were compared in H&E-stained sections of eyes with normal and elevated IOP (Figure 2). Significantly fewer RGCs were present in the right eyes with elevated IOP than the left eyes that did not receive beads (Figure 2A–C). The GCL-NFL/INL ratio was also significantly reduced in eyes with elevated IOP (Figure 2D), reflecting thinning of the GCL-NFL (Figure 2A,D). These results demonstrate that the bead injection induced an increase in high IOP that translated into damaging effects on the retina.

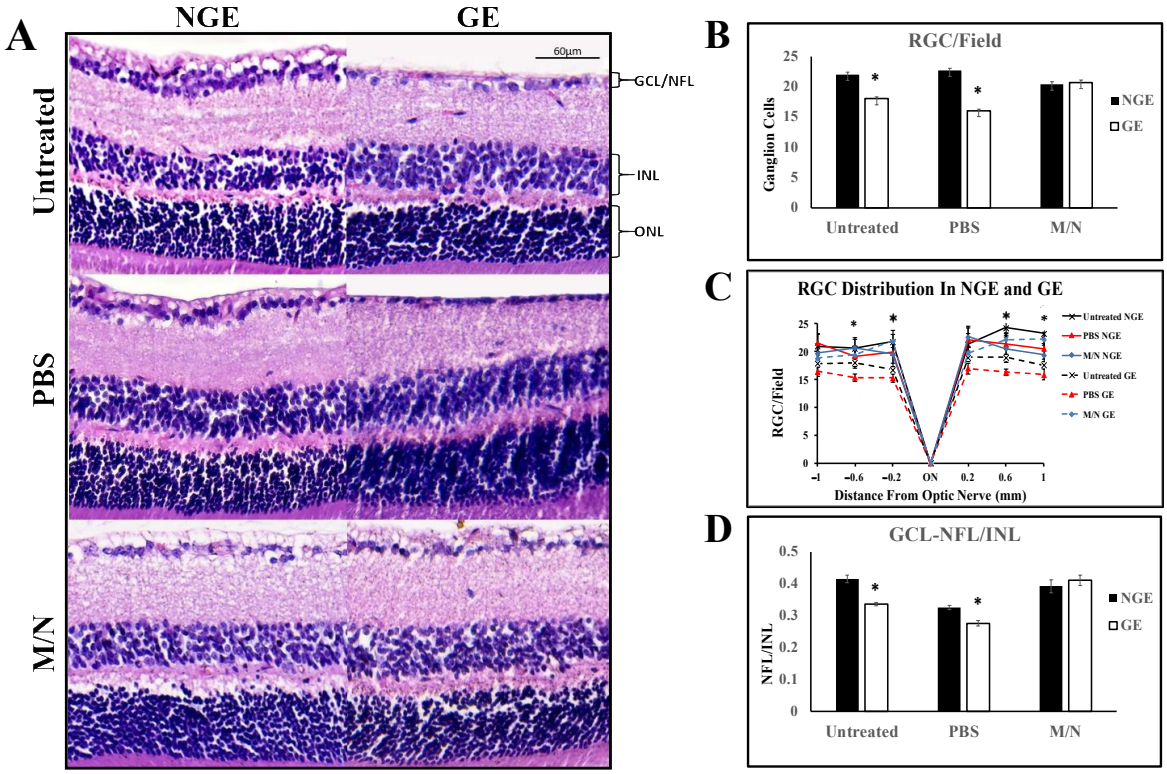

Figure 2. Measurements of RGCs and retinal thickness in glaucomatous vs. non-glaucomatous eyes. (**A**) H&E-stained retinal sections comparing glaucomatous (GEs) and non-glaucomatous eyes (NGEs) in each of the three treatment groups. GCL/NFL, INL, and ONL indicate the ganglion cell layer, the INL, and outer nuclear layer, respectively. Eyes received no injection (untreated), an injection of PBS, or exogenous M/N cells (M/N). High IOP significantly thinned the GCL/NFL, and this was ameliorated by the addition of exogenous M/N cells. (**B**) The total number of RGCs per field in each treatment group in GEs and NGEs. (**C**) The number of RGCs relative to the distance from the optic nerve in each treatment group in eyes with and without bead injections (hatched lines and solid lines, respectively). There was no significant difference between the NGE groups. In the GE groups, statistically significant difference between the M/N-treated group and the untreated and PBS-treated groups is represented by an asterisk (* $p \leq 0.05$). M/N-cell-treated GEs showed more RGCs than those treated with PBS or left untreated. (**D**) GCL/NFL thickness is represented by the GCL-NFL/IFL ratios in each treatment group of GEs and NGEs. GCL-NFL/IFL thickness ratios are shown in all treatments in the NGEs (black bars) and GEs (white bars). Statistically significant difference between the GEs and NGEs within treatment groups is represented by an asterisk (Asterisk means a $p \leq 0.05$). Exogenous treatment of the GEs prevented retinal thinning induced by high IOP.

3.3. Effects of Elevated IOP on the Distribution of Endogenous M/N Cells

Endogenous M/N cells were present in low numbers in the anterior and posterior chambers in non-glaucomatous eyes (NGEs) and had normal IOP, with or without the addition of exogenous M/N cells (Figure 3A). Glaucomatous eyes (GEs) and GEs with PBS showed elevated numbers of endogenous M/N cells throughout the eye on D32 (Figures 3A,B and 4A–Y). Endogenous M/N cells appeared to phagocytose beads around the trabecular meshwork (Figure 4Z–DD)

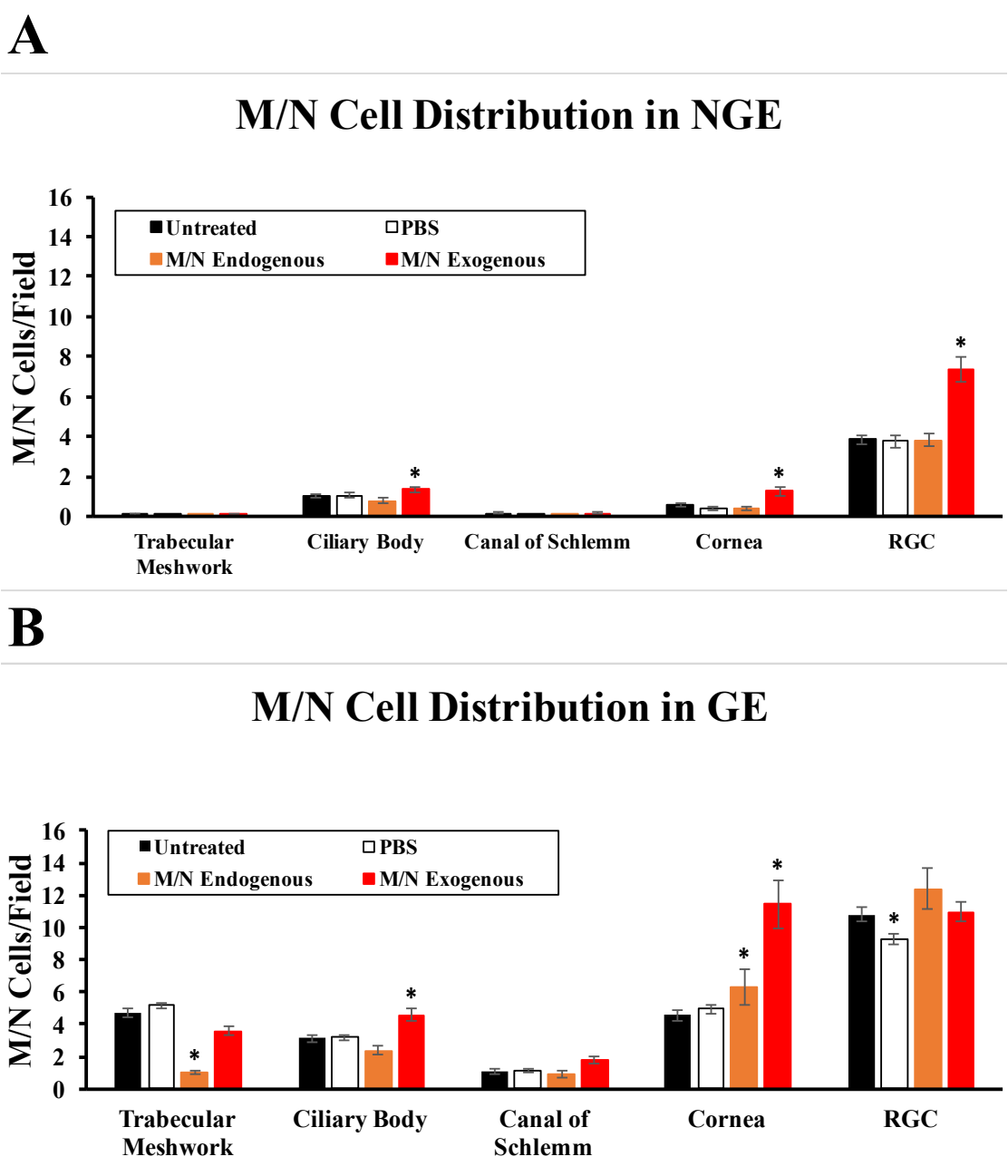

Figure 3. Anatomical distribution of exogeneous and endogenous M/N cells. (**A**,**B**) represent the distribution of endogenous (black, white, and orange bars) and exogenous M/N cells (red bars) on D32 in glaucomatous (GEs) and non-glaucomatous eyes (NGEs) of mice that did not receive an injection of beads (untreated) and that received 2 µL PBS or 2 µL of purified M/N cells (M/N exogenous). Both exogenous and endogenous M/N cells were counted in the GE group that received brain-derived M/N cells. Statistically significant difference from the untreated control group within each area of the eye is represented by an asterisk (* $p \leq 0.05$).

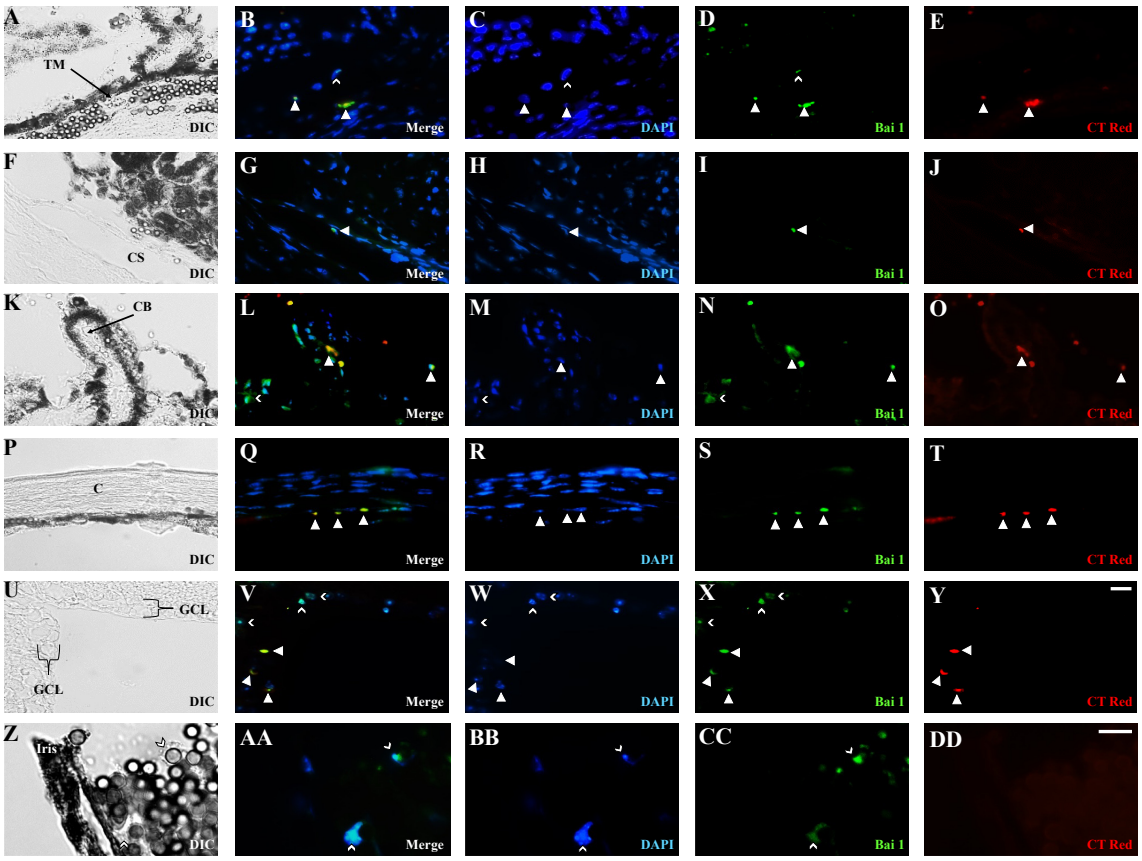

Figure 4. Distribution of M/N cells in glaucomatous mice treated with exogenous M/N cells. Glaucoma was induced by injecting metallic beads into the AC of the mouse eye and positioned at the iridocorneal angle utilizing a magnet. Mice were injected with exogenous M/N cells labeled with CellTracker™ Red (CT Red) 7 days after induction of glaucoma and culled at 32 days. Tissue sections were labeled with Dapi (blue) and G8 BAI1 mAb (green) and imaged with 60× (**A**–**Y**) and 100× lenses (**Z**–**DD**). Chevrons illustrate endogenous M/N cells with green fluorescence only. Triangles illustrate exogenous M/N cells that fluoresced red and green. (**B**,**G**,**L**,**Q**,**V**,**AA**) are merged images of red, green, and blue fluorescence. DIC images show the iris, ciliary body, and microbeads in (**A**,**F**,**K**,**P**,**U**,**Z**), respectively. (**A**–**E**) are images of the trabecular meshwork (TM). The canal of Schlemm (CS) is shown in (**F**). (**K**–**O**) are images of the ciliary body (CB). The cornea (C) is shown in (**P**–**T**). (**U**–**Y**) are images of the ganglion cell layer (GCL). Microbeads present in the cytoplasm of endogenous M/N cells are labeled with chevrons near the iris (**Z**–**CC**). Bar = 9 μm in **A**–**Y** and 4.5 μm in (**Z**–**DD**).

3.4. Distribution of Exogenous M/N Cells in Glaucomatous and Non-Glaucomatous Eyes

The anti-BAI1 G8 mAb was used to isolate M/N cells from the brain [39,46], and the purified cells were injected into the AC of both eyes. Isolated M/N cells were prelabeled with CellTracker™ Red before injection. Exogenous M/N cells were integrated into the anterior and posterior segments of both eyes of non-glaucomatous and glaucomatous eyes (Figure 3A,B). In non-glaucomatous eyes, most of the exogenous M/N cells were integrated into the RGCs, while in the glaucomatous eyes, exogenous M/N cells were found to increase in all ocular tissues analyzed, with the highest increase found in the cornea and the RGC layer (Figures 3 and 4). These analyses demonstrate that the injected M/N cells are viable and able to populate tissues of the anterior and posterior segments in eyes with and without elevated IOP and affect the endogenous population in some areas.

3.5. Effects of Exogenous M/N Cells on Endogenous M/N Cells, IOP, and RGCs

The addition of brain-derived M/N cells significantly decreased the number of endogenous M/N cells in the trabecular meshwork and significantly increased their number in the cornea of glaucomatous eyes (Figures 3A,B and 4P–T) compared to the untreated and PBS groups (Figures 3A,B and 4A–E,P–T). Exogenous M/N cells did not significantly reduce IOP (Figure 1B). However, the addition of M/N cells did significantly reduce cell loss in the GCL, such that the numbers of RGCs were similar in the GEs and NGEs (Figure 2A–C). Exogenous M/N cells also ameliorated the thinning of the NFL in glaucomatous eyes (Figure 2A,D). Thus, increasing the number of M/N cells affects the endogenous population and mitigates the damaging effects of elevated IOP on the retina.

4. Discussion

The loss of ganglion cells in glaucoma eventually leads to blindness. In the case of open-angle glaucoma, blockage of the trabecular meshwork impedes the outflow of aqueous humor [48–50]. There are several characteristics of M/N cells that led us to investigate their behavior in a mouse model of glaucoma. First, they are activated in response to a variety of perturbations in homeostasis, including hypoxia, cell death, incisional and abrasion injuries, and cancer [37–39,41,46,51,52]. Under these conditions, they rapidly accumulate in areas of stress and within wounds. Following injection of microbeads into the AC, M/N cells increase in number in the trabecular meshwork, canal of Schlemm, cornea, and GCL. Brain-derived M/N cells injected into the AC accumulated in the same areas as the endogenous M/N cells. The presence of beads, elevation in IOP, and subsequent tissue damage are likely stimuli for the activation of endogenous M/N cells and homing of both populations of M/N cells to areas of compromise throughout the eye. However, the addition of exogenous cells prevented an increase in endogenous cells in the trabecular meshwork when compared to the no treatment and vehicle control groups in glaucomatous eyes. Apart from the trabecular meshwork, the total number of M/N cells (both exogenous and endogenous) almost doubled compared to the no treatment and vehicle control groups in response to elevated IOP. It is possible that the phagocytosed magnetic beds triggered apoptosis in the M/N cells, thereby lowering their number in this region. The increased number of endogenous Myo/Nog cells in the cornea after injection is probably due to the stress that the injection causes in this tissue and the acute increase in IOP forcing the corneal tissue to stretch, as well as being the location of the injection.

Importantly, M/N cells participated in the clearance of microbeads. M/N cells also ingest tattoo ink in the skin and dead cells in the lens and retina [37,43,53]. We also reported that M/N cells engulf microbeads injected into the AC [53]. It is possible that there were too many beads to clear, even with M/N cell supplementation, to significantly reduce IOP. Furthermore, the polystyrene beads, like tattoo ink, may remain within the cytoplasm of M/N cells once internalized.

Another important characteristic of M/N cells relevant to this study is their ability to protect photoreceptors in oxygen-induced retinopathy and from light damage [38,39]. Their migration to focal wounds in the brain also mitigated cell death [46]. In this mouse model of glaucoma, exogenous M/N cells reduced RGC loss and preserved GCL-NFL thickness in the absence of a significant reduction in IOP. M/N cells' mitigation of RGC loss appears to reflect a neuroprotective effect within the retina, as opposed to a significant drop in IOP, and suggests that their mediation of neuroprotection involves the release of factors within the vitreous and/or the retina itself. Although we assessed RGC numbers using their morphology and nuclear size, we did not label RGCs with a specific antibody against them. Hence, it is possible that in some of the counts that we carried out, Myo/Nog cells, microglia, or astrocytes could have been mistakenly counted. However, the numbers of most of these will increase in stressed tissue. The reduction in cell numbers in the GCL caused by M/N cell injection indicates that it reduced the level of stress in that layer and, likely, the overall number of ganglion cells.

M/N cells' mitigation of RGC loss in this model of glaucoma is predicted to involve multiple mechanisms, including the regulation of the BMP signaling pathway via the release of Noggin. M/N cells are the primary, if not exclusive, source of Noggin throughout the embryo and all adult tissues studied thus far [30,36–40,43,45,46]. Their release of Noggin is critical for normal development of the central nervous system and the eyes [30,36,51]. Implantation of Noggin-soaked beads compensates for the loss of M/N cells during early embryonic development and restores eye morphogenesis [36] Overexpression of Noggin in the brain reduces neuronal cell loss and facilitates neuronal repair in several models of neuronal injury [38,46,54–61].

Like Noggin, BAI1 recognized by G8 mAb, and a commercially available anti-BAI1 mAb appears to be expressed exclusively in M/N cells within the eye [35,38,43,45]. BAI1 is a receptor for phosphatidylserine present on the outer leaflet of the plasma membrane in apoptotic cells and triggers the engulfment process [62]. Examination of the relative contributions of M/N cells and macrophages in maintaining the patency of the trabecular meshwork under normal conditions and in a more slowly progressing model of glaucoma, as well as the relationship between M/N cells and microglia and their roles in clearance in the retina and brain, is warranted. Mechanistic studies are crucial to leveraging M/N cells or the molecules they release for therapeutic purposes in glaucoma and other retinopathies.

Author Contributions: Methodology, P.L., K.J., A.M., J.S.II, J.B., V.M., R.B., N.F., E.W.-L., R.S., E.-J.T., M.M., J.G., G.G., F.D.C., B.H., S.E., M.G.-W. and A.B.-N.; Validation, K.J., R.B., R.S., F.D.C., B.H., M.G.-W. and A.B.-N.; Investigation, P.L., K.J., A.M., J.S.II, J.B., V.M., R.B., S.A., R.S., E.-J.T., M.M., J.G., G.G., S.E. and A.B.-N.; Resources, R.B., M.M. and M.G.-W.; Data curation, P.L., K.J., A.M., J.S.II, R.B., E.W.-L., R.S., F.D.C. and M.G.-W.; Writing—original draft, P.L., N.F., F.D.C., B.H. and A.B.-N.; Writing—review & editing, E.W.-L., S.A., R.S., E.-J.T., J.G., F.D.C., B.H., M.G.-W. and A.B.-N.; Visualization, F.D.C. and B.H.; Supervision, J.G., M.G.-W. and A.B.-N.; Project administration, M.M., F.D.C., B.H. and A.B.-N.; Funding acquisition, A.B.-N. All authors have read and agreed to the published version of the manuscript.

Funding: This research was funded by an anonymous donation for the M/N cell program project to A.B.-N. and M.G.-W, and by and award (DOR 17-22) to A.B.-N. by the Division of Research at the Philadelphia College of Osteopathic Medicine.

Institutional Review Board Statement: All procedures utilized were in accordance with the Association for Research in Vision and Ophthalmology's (ARVO) Statement for the Use of Animals in Ophthalmic and Vision Research and were approved by the Philadelphia College of Osteopathic Medicine's Institutional Animal Care and Use Committee (IACUC). Protocol #A17-012.

Informed Consent Statement: Not applicable.

Data Availability Statement: Data available upon request to corresponding author due to privacy.

Conflicts of Interest: The authors declare no conflict of interest.

Abbreviations

IOP	Intraocular Pressure
AC	Anterior Chamber
BAI1	Brain-Specific Angiogenesis Inhibitor 1
+	Positive
RGC	Retinal Ganglion Cell
NFL/INL	Nerve Fiber Layer/Inner Nuclear Layer

References

1. Parihar, J.K. Glaucoma: The 'Black hole' of irreversible blindness. *Med. J. Armed Forces India* **2016**, *72*, 3–4. [CrossRef] [PubMed]
2. Varma, R.; Peeples, P.; Walt, J.G.; Bramley, T.J. Disease progression and the need for neuroprotection in glaucoma management. *Am. J. Manag. Care* **2008**, *14*, S15–S19. [PubMed]
3. Baudouin, C.; Kolko, M.; Melik-Parsadaniantz, S.; Messmer, E.M. Inflammation in Glaucoma: From the back to the front of the eye, and beyond. *Prog. Retin. Eye Res.* **2021**, *83*, 100916. [CrossRef] [PubMed]

4. Vernazza, S.; Tirendi, S.; Bassi, A.M.; Traverso, C.E.; Sacca, S.C. Neuroinflammation in Primary Open-Angle Glaucoma. *J. Clin. Med.* **2020**, *9*, 3172. [CrossRef] [PubMed]
5. Baudouin, C.; Denoyer, A.; Rostene, W. Glaucoma today: Detection and therapeutic progress. *Biol. Aujourdhui* **2013**, *207*, 87–95. [CrossRef]
6. Anholt, R.R.; Carbone, M.A. A molecular mechanism for glaucoma: Endoplasmic reticulum stress and the unfolded protein response. *Trends Mol. Med.* **2013**, *19*, 586–593. [CrossRef]
7. Fingert, J.H. Primary open-angle glaucoma genes. *Eye* **2011**, *25*, 587–595. [CrossRef]
8. Kwon, Y.H.; Fingert, J.H.; Kuehn, M.H.; Alward, W.L. Primary open-angle glaucoma. *N. Engl. J. Med.* **2009**, *360*, 1113–1124. [CrossRef]
9. Kanagavalli, J.; Pandaranayaka, E.; Krishnadas, S.R.; Krishnaswamy, S.; Sundaresan, P. A review of genetic and structural understanding of the role of myocilin in primary open angle glaucoma. *Indian. J. Ophthalmol.* **2004**, *52*, 271–280.
10. Ray, K.; Mukhopadhyay, A.; Acharya, M. Recent advances in molecular genetics of glaucoma. *Mol. Cell Biochem.* **2003**, *253*, 223–231. [CrossRef]
11. WuDunn, D. Genetic basis of glaucoma. *Curr. Opin. Ophthalmol.* **2002**, *13*, 55–60. [CrossRef] [PubMed]
12. Khazaeni, B.; Khazaeni, L. *Acute Closed Angle Glaucoma*; StatPearls Publishing: Treasure Island, FL, USA, 2023.
13. Dave, S.D.; Meyer, J.J. *Chronic Closed Angle Glaucoma*; StatPearls Publishing: Treasure Island, FL, USA, 2023.
14. Jindra, L.F. Closed-angle glaucoma: Diagnosis and management. *Hosp. Pract.* **1984**, *19*, 114–119. [CrossRef] [PubMed]
15. Mapstone, R. The syndrome of closed-angle glaucoma. *Br. J. Ophthalmol.* **1976**, *60*, 120–123. [CrossRef] [PubMed]
16. Weinreb, R.N.; Aung, T.; Medeiros, F.A. The pathophysiology and treatment of glaucoma: A review. *JAMA* **2014**, *311*, 1901–1911. [CrossRef] [PubMed]
17. Huang, A.S.; Penteado, R.C.; Papoyan, V.; Voskanyan, L.; Weinreb, R.N. Aqueous Angiographic Outflow Improvement after Trabecular Microbypass in Glaucoma Patients. *Ophthalmol. Glaucoma* **2019**, *2*, 11–21. [CrossRef]
18. Ianchulev, T.; Weinreb, R.N.; Kamthan, G.; Calvo, E.; Pamnani, R.; Ahmed, I.K. Biotissue stent for supraciliary outflow in open-angle glaucoma patients: Surgical procedure and first clinical results of an aqueous drainage biostent. *Br. J. Ophthalmol.* **2023**, 1–6. [CrossRef]
19. Evangelho, K.; Mogilevskaya, M.; Losada-Barragan, M.; Vargas-Sanchez, J.K. Pathophysiology of primary open-angle glaucoma from a neuroinflammatory and neurotoxicity perspective: A review of the literature. *Int. Ophthalmol.* **2019**, *39*, 259–271. [CrossRef]
20. Jayaram, H.; Kolko, M.; Friedman, D.S.; Gazzard, G. Glaucoma: Now and beyond. *Lancet* **2023**, *402*, 1788–1801. [CrossRef]
21. Nobl, M.; Priglinger, S.G. Glaucoma—An overview for general practitioners. *MMW Fortschr. Med.* **2023**, *165*, 36–38. [CrossRef]
22. Brazuna, R.; Alonso, R.S.; Salomao, M.Q.; Fernandes, B.F.; Ambrosio, R., Jr. Ocular Biomechanics and Glaucoma. *Vision* **2023**, *7*, 36. [CrossRef]
23. Hsu, E.; Desai, M. Glaucoma and Systemic Disease. *Life* **2023**, *13*, 1018. [CrossRef] [PubMed]
24. Mohan, N.; Chakrabarti, A.; Nazm, N.; Mehta, R.; Edward, D.P. Newer advances in medical management of glaucoma. *Indian J. Ophthalmol.* **2022**, *70*, 1920–1930. [CrossRef] [PubMed]
25. Lusthaus, J.; Goldberg, I. Current management of glaucoma. *Med. J. Aust.* **2019**, *210*, 180–187. [CrossRef] [PubMed]
26. Ito, Y.A.; Belforte, N.; Cueva Vargas, J.L.; Di Polo, A. A Magnetic Microbead Occlusion Model to Induce Ocular Hypertension-Dependent Glaucoma in Mice. *J. Vis. Exp.* **2016**, *109*, e53731. [CrossRef]
27. Samsel, P.A.; Kisiswa, L.; Erichsen, J.T.; Cross, S.D.; Morgan, J.E. A novel method for the induction of experimental glaucoma using magnetic microspheres. *Investig. Ophthalmol. Vis. Sci.* **2011**, *52*, 1671–1675. [CrossRef]
28. Gerhart, J.; Baytion, M.; DeLuca, S.; Getts, R.; Lopez, C.; Niewenhuis, R.; Nilsen, T.; Olex, S.; Weintraub, H.; George-Weinstein, M. DNA dendrimers localize MyoD mRNA in presomitic tissues of the chick embryo. *J. Cell Biol.* **2000**, *149*, 825–834. [CrossRef]
29. Gerhart, J.; Bast, B.; Neely, C.; Iem, S.; Amegbe, P.; Niewenhuis, R.; Miklasz, S.; Cheng, P.F.; George-Weinstein, M. MyoD-positive myoblasts are present in mature fetal organs lacking skeletal muscle. *J. Cell Biol.* **2001**, *155*, 381–392. [CrossRef]
30. Gerhart, J.; Elder, J.; Neely, C.; Schure, J.; Kvist, T.; Knudsen, K.; George-Weinstein, M. MyoD-positive epiblast cells regulate skeletal muscle differentiation in the embryo. *J. Cell Biol.* **2006**, *175*, 283–292. [CrossRef]
31. Strony, R.; Gerhart, J.; Tornambe, D.; Perlman, J.; Neely, C.; Dare, J.; Stewart, B.; George-Weinstein, M. NeuroM and MyoD are expressed in separate subpopulations of cells in the pregastrulating epiblast. *Gene Expr. Patterns* **2005**, *5*, 387–395. [CrossRef]
32. Krause, C.; Guzman, A.; Knaus, P. Noggin. *Int. J. Biochem. Cell Biol.* **2011**, *43*, 478–481. [CrossRef]
33. Secondini, C.; Wetterwald, A.; Schwaninger, R.; Thalmann, G.N.; Cecchini, M.G. The role of the BMP signaling antagonist noggin in the development of prostate cancer osteolytic bone metastasis. *PLoS ONE* **2011**, *6*, e16078. [CrossRef] [PubMed]
34. Wen, L.; Gao, M.; He, Z.; Guo, P.; Liu, Z.; Zhang, P.; Zhang, F.; Chen, D.; Zhou, G.; Zhou, Z. Noggin, an inhibitor of bone morphogenetic protein signaling, antagonizes TGF-beta1 in a mouse model of osteoarthritis. *Biochem. Biophys. Res. Commun.* **2021**, *570*, 199–205. [CrossRef] [PubMed]
35. Gerhart, J.; Bowers, J.; Gugerty, L.; Gerhart, C.; Martin, M.; Abdalla, F.; Bravo-Nuevo, A.; Sullivan, J.T.; Rimkunas, R.; Albertus, A.; et al. Brain-specific angiogenesis inhibitor 1 is expressed in the Myo/Nog cell lineage. *PLoS ONE* **2020**, *15*, e0234792. [CrossRef]
36. Gerhart, J.; Pfautz, J.; Neely, C.; Elder, J.; DuPrey, K.; Menko, A.S.; Knudsen, K.; George-Weinstein, M. Noggin producing, MyoD-positive cells are crucial for eye development. *Dev. Biol.* **2009**, *336*, 30–41. [CrossRef]

37. Gerhart, J.; Greenbaum, M.; Scheinfeld, V.; Fitzgerald, P.; Crawford, M.; Bravo-Nuevo, A.; Pitts, M.; George-Weinstein, M. Myo/Nog cells: Targets for preventing the accumulation of skeletal muscle-like cells in the human lens. *PLoS ONE* **2014**, *9*, e95262. [CrossRef] [PubMed]
38. Bravo-Nuevo, A.; Brandli, A.A.; Gerhart, J.; Nichols, J.; Pitts, M.; Sutera, C.K.; Assali, S.; Scheinfeld, V.; Prendergast, G.C.; Stone, J.; et al. Neuroprotective effect of Myo/Nog cells in the stressed retina. *Exp. Eye Res.* **2016**, *146*, 22–25. [CrossRef]
39. Brandli, A.; Gerhart, J.; Sutera, C.K.; Purushothuman, S.; George-Weinstein, M.; Stone, J.; Bravo-Nuevo, A. Role of Myo/Nog Cells in Neuroprotection: Evidence from the Light Damaged Retina. *PLoS ONE* **2017**, *12*, e0169744. [CrossRef]
40. Gerhart, J.; Withers, C.; Gerhart, C.; Werner, L.; Mamalis, N.; Bravo-Nuevo, A.; Scheinfeld, V.; FitzGerald, P.; Getts, R.; George-Weinstein, M. Myo/Nog cells are present in the ciliary processes, on the zonule of Zinn and posterior capsule of the lens following cataract surgery. *Exp. Eye Res.* **2018**, *171*, 101–105. [CrossRef]
41. Gerhart, J.; Behling, K.; Paessler, M.; Milton, L.; Bramblett, G.; Garcia, D.; Pitts, M.; Hurtt, R.; Crawford, M.; Lackman, R.; et al. Rhabdomyosarcoma and Wilms tumors contain a subpopulation of noggin producing, myogenic cells immunoreactive for lens beaded filament proteins. *PLoS ONE* **2019**, *14*, e0214758. [CrossRef]
42. Gerhart, J.; Greenbaum, M.; Casta, L.; Clemente, A.; Mathers, K.; Getts, R.; George-Weinstein, M. Antibody-Conjugated, DNA-Based Nanocarriers Intercalated with Doxorubicin Eliminate Myofibroblasts in Explants of Human Lens Tissue. *J. Pharmacol. Exp. Ther.* **2017**, *361*, 60–67. [CrossRef]
43. Gerhart, J.; Werner, L.; Mamalis, N.; Infanti, J.; Withers, C.; Abdalla, F.; Gerhart, C.; Bravo-Nuevo, A.; Gerhart, O.; Getts, L.; et al. Depletion of Myo/Nog Cells in the Lens Mitigates Posterior Capsule Opacification in Rabbits. *Investig. Ophthalmol. Vis. Sci.* **2019**, *60*, 1813–1823. [CrossRef] [PubMed]
44. Gerhart, J.; Morrison, N.; Gugerty, L.; Telander, D.; Bravo-Nuevo, A.; George-Weinstein, M. Myo/Nog cells expressing muscle proteins are present in preretinal membranes from patients with proliferative vitreoretinopathy. *Exp. Eye Res.* **2020**, *197*, 108080. [CrossRef]
45. Crispin, M.; Gerhart, J.; Heffer, A.; Martin, M.; Abdalla, F.; Bravo-Nuevo, A.; Philp, N.J.; Kuriyan, A.E.; George-Weinstein, M. Myo/Nog Cells Give Rise to Myofibroblasts During Epiretinal Membrane Formation in a Mouse Model of Proliferative Vitreoretinopathy. *Investig. Ophthalmol. Vis. Sci.* **2023**, *64*, 1. [CrossRef] [PubMed]
46. Joseph-Pauline, S.; Morrison, N.; Braccia, M.; Payne, A.; Gugerty, L.; Mostoller, J.; Lecker, P.; Tsai, E.J.; Kim, J.; Martin, M.; et al. Acute Response and Neuroprotective Role of Myo/Nog Cells Assessed in a Rat Model of Focal Brain Injury. *Front. Neurosci.* **2021**, *15*, 780707. [CrossRef] [PubMed]
47. Chu, A.J.; Zhao, E.J.; Chiao, M.; Lim, C.J. Co-culture of induced pluripotent stem cells with cardiomyocytes is sufficient to promote their differentiation into cardiomyocytes. *PLoS ONE* **2020**, *15*, e0230966. [CrossRef]
48. Ferrer, E. Trabecular meshwork as a new target for the treatment of glaucoma. *Drug News Perspect.* **2006**, *19*, 151–158. [CrossRef]
49. Gong, H.; Freddo, T.F. The washout phenomenon in aqueous outflow--why does it matter? *Exp. Eye Res.* **2009**, *88*, 729–737. [CrossRef]
50. Braunger, B.M.; Fuchshofer, R.; Tamm, E.R. The aqueous humor outflow pathways in glaucoma: A unifying concept of disease mechanisms and causative treatment. *Eur. J. Pharm. Biopharm.* **2015**, *95*, 173–181. [CrossRef]
51. Gerhart, J.; Scheinfeld, V.L.; Milito, T.; Pfautz, J.; Neely, C.; Fisher-Vance, D.; Sutter, K.; Crawford, M.; Knudsen, K.; George-Weinstein, M. Myo/Nog cell regulation of bone morphogenetic protein signaling in the blastocyst is essential for normal morphogenesis and striated muscle lineage specification. *Dev. Biol.* **2011**, *359*, 12–25. [CrossRef]
52. Gerhart, J.; Hayes, C.; Scheinfeld, V.; Chernick, M.; Gilmour, S.; George-Weinstein, M. Myo/Nog cells in normal, wounded and tumor-bearing skin. *Exp. Dermatol.* **2012**, *21*, 466–468. [CrossRef]
53. Gerhart, J.; Gugerty, L.; Lecker, P.; Abdalla, F.; Martin, M.; Gerhart, O.; Gerhart, C.; Johal, K.; Bernstein, J.; Spikes, J.; et al. Myo/Nog cells are nonprofessional phagocytes. *PLoS ONE* **2020**, *15*, e0235898. [CrossRef] [PubMed]
54. Samanta, J.; Alden, T.; Gobeske, K.; Kan, L.; Kessler, J.A. Noggin protects against ischemic brain injury in rodents. *Stroke* **2010**, *41*, 357–362. [CrossRef] [PubMed]
55. Xiao, Q.; Du, Y.; Wu, W.; Yip, H.K. Bone morphogenetic proteins mediate cellular response and, together with Noggin, regulate astrocyte differentiation after spinal cord injury. *Exp. Neurol.* **2010**, *221*, 353–366. [CrossRef] [PubMed]
56. Dizon, M.L.; Maa, T.; Kessler, J.A. The bone morphogenetic protein antagonist noggin protects white matter after perinatal hypoxia-ischemia. *Neurobiol. Dis.* **2011**, *42*, 318–326. [CrossRef] [PubMed]
57. Ma, C.H.; Brenner, G.J.; Omura, T.; Samad, O.A.; Costigan, M.; Inquimbert, P.; Niederkofler, V.; Salie, R.; Sun, C.C.; Lin, H.Y.; et al. The BMP coreceptor RGMb promotes while the endogenous BMP antagonist noggin reduces neurite outgrowth and peripheral nerve regeneration by modulating BMP signaling. *J. Neurosci.* **2011**, *31*, 18391–18400. [CrossRef] [PubMed]
58. Gulino, R.; Gulisano, M. Noggin and Sonic hedgehog are involved in compensatory changes within the motoneuron-depleted mouse spinal cord. *J. Neurol. Sci.* **2013**, *332*, 102–109. [CrossRef] [PubMed]
59. Hashimoto, M.; Koda, M.; Furuya, T.; Murata, A.; Yamazaki, M.; Takahashi, K. Intrathecal Noggin administration in rats temporally ameliorates mechanical allodynia induced by a chronic constriction injury. *eNeurologicalSci* **2016**, *4*, 4–9. [CrossRef]
60. Al-Sammarraie, N.; Mahmood, M.; Ray, S.K. Neuroprotective role of Noggin in spinal cord injury. *Neural Regen. Res.* **2023**, *18*, 492–496. [CrossRef]

61. Su, X.; Ying, J.; Xiao, D.; Qiu, X.; Li, S.; Zhao, F.; Tang, J. Activin A rescues preterm brain injury through a novel Noggin/BMP4/Id2 signaling pathway. *Int. J. Mol. Med.* **2023**, *51*, 12. [CrossRef]
62. Park, D.; Tosello-Trampont, A.C.; Elliott, M.R.; Lu, M.; Haney, L.B.; Ma, Z.; Klibanov, A.L.; Mandell, J.W.; Ravichandran, K.S. BAI1 is an engulfment receptor for apoptotic cells upstream of the ELMO/Dock180/Rac module. *Nature* **2007**, *450*, 430–434. [CrossRef]